

1 **Comparison of slant open-path flux gradient and static closed chamber techniques to**
2 **measure soil N₂O emissions**

3 Mei Bai^{1,*}, Helen Suter¹, Shu Kee Lam¹, Thomas K. Flesch², Deli Chen¹

4 ¹Faculty of Veterinary and Agricultural Sciences, The University of Melbourne, Parkville, VIC
5 3010, Australia

6 ²Department of Earth and Atmospheric Sciences, University of Alberta, Edmonton, AB T6E
7 2H4, Canada

8 *Correspondence to:* Mei Bai (mei.bai@unimelb.edu.au)

9

10 **Abstract**

11 Improving direct field measurement techniques to quantify gases emissions from cropped
12 agricultural fields is challenging. We compared nitrous oxide (N₂O) emissions measured with
13 static closed chambers to those from a newly developed aerodynamic flux gradient (FG)
14 approach. Measurements were made at a vegetable farm following chicken manure application.
15 The FG calculations were made with a single open-path Fourier transform infrared (OP-FTIR)
16 spectrometer (height of 1.45 m) deployed in a slant-path configuration: sequentially aimed at
17 retro reflectors at heights of 0.8 and 1.8 m above ground. Hourly emissions were measured
18 with the FG technique, but once a day between 10:00 and 13:00 with chambers. We compared
19 the concurrent emission ratios (FG/Chambers) between these two techniques, and found N₂O
20 emission rates from celery crop farm measured at mid-day by FG were statistically higher
21 (1.22–1.40 times) than those from the chambers measured at the same time. Our results suggest
22 the OP-FTIR slant-path FG configuration worked well in this study: it was sufficiently sensitive
23 to detect the N₂O gradients over our site, giving high temporal resolution N₂O emissions
24 corresponding to a large measurement footprint.

25

26 **Keywords:** chamber techniques, chicken manure, flux gradient, N₂O emission, OP-FTIR
27 spectroscopy

28

29 **Abbreviations:** FG, flux gradient; OP-FTIR, open-path Fourier transform infrared
30 spectroscopy

31

32 **1 Introduction**

33 The accurate measurement of soil nitrous oxide (N₂O) emissions from agricultural land is
34 challenging. Chambers are commonly used for these measurements (Hutchinson and Mosier,
35 1981), and chamber based observations are widely used to calculate greenhouse gas inventories
36 (Dalal et al., 2008). The principle behind the most common type of chamber measurement
37 (static, or non-steady state) is to create a sealed control volume over the soil surface, such that
38 by monitoring the gas concentration change during the chamber deployment, one can calculate
39 the surface emission rate (Denmead, 2008). One of the advantages of chambers is that they can
40 be employed at relatively low cost, with simplicity and easy field operation (de Klein et al.,
41 2001). However, chambers have a fundamental limitation – the control volume inevitably
42 perturbs the soil-atmosphere interface (e.g., temperature, pressure), which has the potential to
43 modify the ambient soil emission rate (Denmead, 1979). Moreover, manually operated static
44 chambers are not well-suited to measure temporal variations in emissions (Denmead et al.,
45 2008; Jones et al., 2011). The temporal variation issue can be addressed by alternative
46 approaches, e.g. a dynamic measurement with automated-chamber opening and closing by
47 pneumatic actuators (Yao et al., 2009) and can be run for many months. However, in many
48 situations the most important disadvantage of chambers is their small surface measurement
49 footprint. With a surface enclosure typically less than 1 m², and the likelihood that soil
50 emissions vary dramatically at length scales greater than 1 m (Denmead, 2008; Griffith and

51 Galle, 2000; Turner et al., 2008), many replications are needed to adequately quantify the
52 emissions from an agricultural field (Christensen et al., 1996; Denmead, 1995).

53

54 Micrometeorological measurements avoid some of the problems associated with chamber
55 methods (Christensen et al., 1996; Denmead et al., 2010; Li et al., 2008; Pattey et al., 2006).

56 These techniques are based on concentration and windflow measurements made in the free air
57 above the surface, and they do not perturb the surface environment. They also measure
58 emissions over footprints much larger than those from chambers (Hargreaves et al., 1996). The
59 aerodynamic flux gradient (FG) technique is a well-used micrometeorological method, where
60 the vertical flux of gas is inferred from a height gradient in concentration (multiplied by an
61 estimate of the turbulent diffusivity). When measured above a large and homogeneous surface,
62 this atmospheric flux is assumed equal to the underlying surface emission or absorption rate.

63 In this study we used a recently developed modification of the technique. Rather than vertically
64 separated point concentrations, we used a slant-path configuration based on vertically separated
65 long line-averaged measurements (Flesch et al., 2016; Wilson and Flesch, 2016). A single
66 open-path Fourier transform infrared (OP-FTIR) concentration sensor with motorized aiming
67 gives the gas concentrations along the two paths, from which we can calculate the surface
68 emission/deposition rate.

69

70 In this study we conducted a set of N₂O emission measurements from a vegetable farm
71 following manure application. Measurements were made with both static chambers and the
72 slant-path FG approach. Our objective was to 1) demonstrate the newly developed slant-path
73 FG method at a vegetable farm; and 2) compare the emission rates measured by the static
74 chamber and FG techniques.

75

76 **2 Materials and methods**

77 **2.1 Experimental site**

78 This study was conducted at an intensive vegetable farm in Clyde, Victoria, Australia (38.1°
79 S, 145.3° E). The site consisted of two adjacent fields of 5.4 ha (Site 1) and 3.1 ha (Site 2).
80 These sites differ only in the addition of a fertilizer amendment at Site 2. A celery crop at the
81 4-5 leaf stage was transplanted to these two sites on 27 February 2014 (Fig. 1). Chicken manure
82 (4.3% N, $\text{NH}_4^+\text{-N}$: 4633 mg kg⁻¹, $\text{NO}_3\text{-N}$: 313 mg kg⁻¹) was applied at rate of 8.2 tonne ha⁻¹ at
83 both sites on 28 March. Fertiliser Cal-Gran (a blend of calcium ammonium nitrate and
84 ammonium sulphate, total 23.9% N) was also applied at both sites at rate of 200 kg ha⁻¹ on 15
85 April. Emission measurements began just prior to manure application and ended on 6 May
86 2014. The terrain was open and flat with sandy loam topsoils. Prevailing winds were southeast
87 or northwest during this period. The average daily minimum and maximum temperature were
88 6 and 33°C, respectively. The total precipitation (including rainfall and irrigation) during the
89 measurement period was 186 mm.

90 Figure 1

91

92 **2.2 Methodologies**

93 **2.2.1 Static chamber**

94 Four static chambers (50 × 50 × 25 cm) were located at each site (Fig. 1). The metal base for
95 each chamber was placed into the soil to a depth of 8 cm prior to the experiment, and remained
96 in place through the study. The chamber was made of plexiglass with a built in ventilation
97 system. Reflective aluminium foil was attached inside the lid to minimize changes in ambient
98 pressure and temperature after the chamber was placed onto the base. A thermocouple Tinytag
99 Transit 2 (TG-4080 temperature loggers, West Sussex, UK) was placed on the soil surface
100 inside the chamber to monitor the headspace air temperature. Gas samples (20 mL) were

101 collected into evacuated 12 mL vials (Exetainer®, Labco Ltd., Ceredigion, UK) at 0, 30 and
 102 60 minutes after chamber placement and analysed at an off-site laboratory by gas
 103 chromatography (GC) (Agilent 7890A, Wilmington, USA). The sensitivity of GC for N₂O
 104 concentration was 0.01 ppm. Gas samples were collected daily between 10:00 and 13:00 from
 105 29 March to 7 April and on 9, 11 and 16 April. The N₂O flux was calculated as (Ruser et al.,
 106 1998) (Eq. 1):

$$107 \quad Q_{chamber} = K_{N_2O} (273/T) (V/A) dC/dt \quad (1)$$

108 where $Q_{chamber}$ is the gas flux ($\mu\text{g N}_2\text{O-N m}^{-2} \text{ h}^{-1}$); K_{N_2O} is 1.25 ($\mu\text{g N } \mu\text{L}^{-1}$) according to the
 109 ideal gas law, where $K_{N_2O} = P m/R T_0$, and P is air pressure (at 1 atm), m is molecular mass (28
 110 g mol^{-1}), R is gas constant ($0.0821 \text{ L atm K}^{-1} \text{ mol}^{-1}$), and T_0 is 273 K; T is the air temperature
 111 within the chamber (K); V is the total volume of headspace (L); A is a surface area inside the
 112 chamber (m^2); and dC/dt is the rate of change in mole fraction of N₂O in the chamber ($\mu\text{L L}^{-1}$
 113 h^{-1}) determined by linear regression model. The N₂O mole fraction is provide by GC, in ppm.
 114

115 **2.2.2 Flux gradient**

116 The basic principle of the FG method has been well-described (Judd et al., 1999; Laubach and
 117 Kelliher, 2004; Webb et al., 1980). We followed a modification described in Flesch et al.
 118 (2016), in which an open-path sensor was used to measure the concentration difference (ΔC_L)
 119 between two vertically offset slant-paths. The open-path sensor measures gas concentration
 120 between the sensor and a distant retro reflector. The concentration difference ΔC_L is calculated
 121 by sequentially aiming the sensor at high and low retro reflectors. Flesch et al. (2016) showed
 122 that the conventional FG equation can be transformed into Eqs. 2, 3:

$$123 \quad Q_{FG} = (k_v \rho_a u^*/S_c)(M_s/M_a) * \kappa * \Delta C_L \quad (2)$$

$$124 \quad \kappa = l_{PATH} / \int_{x_1}^{x_2} [\ln(z_{p2}/z_{p1}) - \phi(z_{p2}/L) + \phi(z_{p1}/L)] dx \quad (3)$$

125 where Q_{FG} is the gas flux ($\text{g m}^{-2} \text{s}^{-1}$), k_v is von Karman's constant (0.4), ρ_a is dry air density (g
126 m^{-3}), u^* is friction velocity (m s^{-1}), S_c is the turbulent Schmidt number (0.64), M_s and M_a are
127 the molar mass of N_2O (44 g mol^{-1}) and dry air (29 g mol^{-1}), respectively, ΔC_L (ppb) is the
128 difference in the line-average volumetric mixing ratio of the gas (relative to dry air) from the
129 lower (z_{p1}) and upper (z_{p2}) paths (m, relative to celery beds surface), κ is proportional to the
130 height integral of the gas diffusivity along the FTIR path pair, l_{PATH} is the sensor-retro reflector
131 path length (m, equal for the two paths), L is atmospheric Obukhov stability length (m). Path
132 heights (z_{p1} and z_{p2}) along the path length are given by a 5th-order polynomial fit of height vs.
133 distance from the OP-FTIR spectrometer (path heights were measured in the field at 5 m
134 intervals). We used the stability correction factor φ from Flesch et al. (2016).

135

136 An estimate of the uncertainty in Q_{FG} (δQ_{FG}) was calculated as the sum in quadrature of the
137 relative uncertainties in S_c , ΔC_L and κ according to the formula described in Flesch et al. (2016).
138 Q_{FG} values were not calculated when $u^* < 0.05 \text{ m s}^{-1}$.

139

140 The FG calculations relied on open-path concentrations measured with a robust Bruker OP-
141 FTIR spectrometer (Matrix-M IRcube, Bruker Optics, Ettlingen, Germany) and two retro
142 reflectors located 80 m from the spectrometer (PLX Industries, New York, USA). Briefly, the
143 OP-FTIR system measures multiple gas concentrations (N_2O , CH_4 , NH_3 , CO_2 , CO and water
144 vapour) with high precision ($\text{N}_2\text{O} < 0.3 \text{ ppb}$, $\text{CH}_4 < 2 \text{ ppb}$, NH_3 , 0.4 ppb , CO_2 , 1 ppm , CO , 0.1
145 ppb , and water vapour $< 5\%$) (Griffith, 1996; Griffith et al., 2008; Griffith et al., 2012). More
146 details on the OP-FTIR system can be found in Bai (2010). The spectrometer was mounted at
147 a height of 1.45 m above ground. A motorized mounting head sequentially aimed the
148 spectrometer to the retro reflectors at 0.8 and 1.8 m above ground. Line-averaged N_2O
149 concentrations with an averaging time of 2.5-min were measured. Background N_2O

150 concentrations were measured prior to manure application in order to assess measurement
151 precision. A sequence of observations were averaged, the standard deviation of the mean was
152 retrieved and the precision of N₂O concentration measurements (less than 0.3 ppb) was
153 determined according to Bai (2010). The OP-FTIR measurements were made continuously
154 from 25 March until 16 April, and thereafter measurements were made for three days
155 (continuously) per week until 6 May.

156

157 A weather station coupled with a three-dimensional sonic anemometer (CSAT3, Campbell
158 Scientific, Logan, UT, USA) was established at a height of 3.0 m above ground, 50 m east of
159 Site 2. Fifteen-min average climatic data including ambient temperature, pressure and wind
160 statistics were recorded by a data logger (CR23X, Campbell Scientific, Logan, UT, USA) at a
161 frequency of 10 Hz. Atmospheric stability parameters of friction velocity (u^*), surface
162 roughness (z_0) and Obukhov stability length (L) were calculated from the ultrasonic
163 anemometer data. We used a data filtering procedure to remove error-prone observations in the
164 FG calculation according to Flesch et al. (2014).

165

166 The FG flux measurements correspond to surface emissions within a flux “footprint”. The
167 footprint generally extends upwind of the concentration sensors, but its spatial size varies with
168 wind conditions. A concern of this study is that the FG footprint extends beyond our plots, and
169 the calculated emission rates are “contaminated” by emissions occurring outside the plot. This
170 possibility was investigated by modelling the FG footprint for our smaller Site 2, where the
171 contamination concerns are greater. The WindTrax dispersion software
172 (thunderbeachscientific.com) was used to simulate the OP-FTIR slant-path setup, and calculate
173 the fraction of the FG measured flux occurring within the Site 2 plot. We looked at the wind
174 direction that results in a short fetch (NE), and looked at different atmospheric stability

175 conditions and roughness lengths. The results for $z_0 = 0.1$ m (representative of the plot) are
176 shown in Figure 2. We concluded that during stable night-time conditions the FG emission
177 calculations for Site 2 maybe contaminated by up to 40% by outside fluxes. This may result in
178 either over- or under-estimation of Site 2 emissions depending on the emission rate outside the
179 plot. In unstable daytime conditions the contamination potential falls to 0–10%. Contamination
180 at Site 1 will not be as serious due to the larger fetches.

181

182 The main objective of our study is to compare chamber and FG emission estimates. We looked
183 at periods with concurrent measurements from the two techniques, and hourly flux ratios of
184 $Q_{FG}/Q_{chamber}$ measured between 10:00 and 13:00 are compared. Because the comparison took
185 place during the day when conditions were generally unstable, the FG contamination potential
186 is low (and will be ignored). The contamination potential does highlight a concern with
187 micrometeorological measurements, that a large measurement footprint may extend outside the
188 study area and result in measurement errors.

189 Figure 2

190

191 **3 Results and discussion**

192 **3.1 Daily N₂O flux**

193 The FG measurements gave high temporal resolution of fluxes and this provides an opportunity
194 to study the pattern of N₂O emissions in detail. Here we only describe the temporal flux
195 measurements from Site 1.

196

197 **3.1.1 The flux gradient fluxes**

198 Hourly N₂O fluxes showed large temporal variation during the experimental period in response
199 to fertilisation. There was a rapid increase in N₂O emission from a background level of 0.6 mg

200 $\text{N}_2\text{O-N m}^{-2} \text{ h}^{-1}$ before manure application to a peak of $158.0 \text{ mg N}_2\text{O-N m}^{-2} \text{ h}^{-1}$ within 24 h
201 after application, which could be attributed to both nitrification and denitrification. After the
202 peak, several spikes between 16–17 April were also observed associated with fertilizer
203 application, followed by a decline in emissions to an average of $2.5 \text{ mg N}_2\text{O-N m}^{-2} \text{ h}^{-1}$ (Fig.
204 3A). One of the conclusions we draw from Figure 3B is that the slant path FG system is
205 sensitive enough to measure the N_2O fluxes that accompanied fertilisation at our site, i.e., the
206 measurement uncertainty as represented by $1-\sigma$ is generally well below the flux magnitude.

207

208 In addition to the long-term pattern of decreasing emissions after manure application, we
209 observed a diurnal pattern where maximum emission tended to occur in the late afternoon
210 (16:00) (Fig. 3B). We believe this is related to the time of maximum soil surface temperature,
211 which occurs after the peak air temperature (Christensen et al., 1996; Wang et al., 2013). A
212 strong diurnal emission pattern implies that once-a-day snapshot emission measurements (e.g.,
213 chambers) would almost certainly give a biased estimate of the daily average emission rate.
214 We also noticed occasional high emissions at night, which was closely related to precipitation
215 events. Negative N_2O fluxes calculated from the FG measurements most likely represent
216 instrument noise, as the flux magnitudes were below the detectable limit of our OP-FTIR
217 system, i.e., the uncertainty represented by the $1-\sigma$ error bars in Fig. 3 span zero.

218 Figure 3

219

220 **3.1.2 Chamber fluxes**

221 Nitrous oxide fluxes from the static chambers (once-a-day snapshots) were in general
222 agreement with the FG measurements in terms of the long-term background exchange patterns
223 (Fig. 3): hourly fluxes rose from a background level of $1.12 \text{ mg N}_2\text{O-N m}^{-2} \text{ h}^{-1}$ (before manure
224 application, data is not shown), reached a spike of $3.48 \text{ mg N}_2\text{O-N m}^{-2} \text{ h}^{-1}$ 48 hours after

225 manure application, then dropped to a minimum of 1.02 mg N₂O–N m⁻² h⁻¹ on 5 April. A
226 maximum emission peak of 3.55 mg N₂O–N m⁻² h⁻¹ was measured on 16 April and was most
227 likely related to fertilizer application.

228

229 **3.2 Comparison of the two measurement techniques**

230 We selected the concurrent measurements from FG and the chambers and a total of 23
231 comparison pairs were obtained during the study period (note that each chamber observation
232 is an average from four replicate chambers). We calculated the ratio $Q_{FG}/Q_{chamber}$ of these
233 concurrent pairs.

234

235 The $Q_{FG}/Q_{chamber}$ ratio showed large variation, with values ranging between 0.4 and 4.9. The
236 $Q_{FG}/Q_{chamber}$ data follows a non-normal distribution. To better interpret these data we log-
237 transformed the ratios (Abdi et al., 2015). The average of the natural logarithm of the ratio,
238 converted back to the ratio units, gives the geometric mean (the process was duplicated to
239 calculate the confidence interval $\alpha = 0.9$). The geometric mean of $Q_{FG}/Q_{chamber}$ was 1.40, with
240 a confidence interval ranging from 1.15 to 1.69. This means that on average the FG measured
241 fluxes were 40% higher than those from the chambers, and this difference was statistically
242 significant.

243

244 Differences between chamber and micrometeorological measurements have been previously
245 noted. Some studies have reported that micrometeorological techniques gave emission rates
246 that were 50–60% of those from chambers (Christensen et al., 1996; Neftel et al., 2010). In
247 contrast, Wang et al. (2013) reported N₂O emissions measured by chambers were 17–20%
248 lower than from the eddy covariance micrometeorological technique, and Norman et al. (1997)
249 reported that chamber measurements were 30% lower than micrometeorological

250 measurements. Sommer et al. (2004) found static vented chambers underestimated N₂O
251 emissions from manure piles by 12–22% compared to mass balance measurements.

252

253 Discrepancies between FG and chamber fluxes could be due to very different measurement
254 footprints. Large spatial variability is a characteristic of soil N₂O emissions. For example,
255 Turner et al. (2008) reported N₂O emissions varied from 30 to 800 ng N₂O–N m⁻² s⁻¹ over an
256 irrigated dairy pasture (8,100 m²). This high variability, together with the substantial difference
257 in measurement footprint size (chambers < 1 m² vs FG > 1000 m²) will likely result in
258 differences between the two techniques because the chambers are not capable of accounting
259 for this variability, unless many chambers are used, whilst the FG method can. If this explains
260 the difference between the two techniques, then discrepancies between chambers and
261 micrometeorological techniques should be site dependent, i.e., dependent on the degree of
262 spatial variability in emissions at each site.

263

264 Several researchers have reported that chamber flux calculation procedures introduced large
265 uncertainty in N₂O emissions (Levy et al., 2011; Venterea et al., 2010). In particular, using
266 linear regression to determine the rate of change dC/dt in Eq. (1) can lead to an underestimate
267 of emissions (Anthony et al., 1995; Matthias et al., 1978). Venterea (2013) concluded that the
268 typical calculations used for non-steady state chambers underestimated N₂O emissions by
269 20–50%. To examine the potential bias in N₂O emissions when dC/dt is estimated with a linear
270 regression model, we also calculated the results using a non-linear monomolecular model
271 (Bolker, 2007). The monomolecular model is one of the simplest saturating functions and
272 follows (Eq. 4):

273
$$C_{N_2O} = a_0 + a_1 (1 - \exp(-a_2/a_1 * t)) \quad (4)$$

274 where C_{N_2O} is the mole fraction of N_2O , a_0 is the intercept corresponding to the N_2O mole
275 fraction at time $t = 0$, a_1 is the horizontal asymptote at $t = +\infty$, a_2 is the slope (dC/dt) at $t = 0$,
276 and t is time after chamber placement (h).

277

278 Chamber fluxes calculated using the non-linear dC/dt ($Q_{\text{chamber-non-linear}}$) were 1.15 times higher
279 than Q_{chamber} estimated using linear regression. Comparing the concurrent fluxes of Q_{FG} and
280 $Q_{\text{chamber-non-linear}}$, we found the geometric mean of $Q_{\text{FG}}/Q_{\text{chamber-non-linear}}$ to be 1.22 (confidence
281 interval of 0.99 to 1.49). Using 10,000 bootstrap re-samples (Efron and Tibshirani, 1994), we
282 computed 10,000 potential mean fluxes from the non-linear model, of which 9540 of the means
283 were greater than 1, and 460 were lower than 1. This result suggests the use of the non-linear
284 dC/dt calculation has resulted in better agreement with the FG estimates.

285

286 While there is a long and successful history of FG applications, there are still questions about
287 its implementation. The value of the turbulent Schmidt number (Sc) in Eq. (2) is debated (Flesch
288 et al., 2002). There is also a concern regarding the accuracy of FG during light winds. In our
289 study the light wind data ($0.05\text{--}0.15\text{ m s}^{-1}$) accounted for 24% of the measurement periods. We
290 found the FG uncertainty ($\delta_{Q_{\text{FG}}}/Q_{\text{FG}}$) increased from 0.41 to 1.25 when the friction velocity (u^*)
291 dropped from 0.15 to 0.05 m s^{-1} . However, we note that in this study the periods in which we
292 compared FG and chamber measurements were not light wind periods.

293

294 Using the FG method, we estimated that the cumulative N_2O emissions over the 41-day
295 observation period were 14.6 kg N ha^{-1} , corresponding to 3.7% of total applied N.

296

297 **4 Conclusions**

298 Our results showed that soil N₂O emissions measured by FG and static chambers (linear dC/dt)
299 were statistically different, with fluxes from FG being on average 40% higher. Using a non-
300 linear calculation of dC/dt in the chambers decreased the disagreement to 22%. Given the
301 likelihood of large spatial variability in N₂O emissions, and the vastly different measurement
302 footprints of the two methods, it is not surprising the two techniques give different results. It is
303 difficult to conclude that one technique or the other is biased based on this experiment alone.
304 However, the relationship we observed, together with other reports on the biases created by
305 chamber calculation procedures, supports an interpretation that our FG emission calculations
306 were accurate and in this instance the chamber measurements were biased too low.

307

308 The OP-FTIR flux gradient system used here showed the capability for real-time emission
309 measurements over a large spatial footprint with no surface interference. Furthermore, being
310 free from pumps and tubing, the open-path FG system would be particularly advantageous for
311 measuring multiple gas emissions including “sticky” gases like NH₃.

312

313 **5 Author contribution**

314 DC, HS, SKL, MB and TF designed the experiments and MB and SKL carried them out. TF
315 and MB developed the techniques. MB prepared the manuscript with contributions from all
316 co-authors.

317

318 **6 Competing interests**

319 The authors declare that they have no conflict of interest.

320

321 **7 Acknowledgments**

322 This study was funded by the Australian Department of Agriculture (DA), and the Canadian
323 Agricultural Greenhouse Gases Program (AGGP). The authors thank Schruers' vegetable farm,
324 Adam Schruers and staff for their great support. The authors also thank Rohan Davies from
325 BASF Australia Ltd. for providing assistance. We gratefully acknowledge the assistance of the
326 staff and students from Faculty of Veterinary and Agricultural Sciences soil research group at
327 the University of Melbourne during this campaign. We specially thank Dr Raphaël Trouvé for
328 helping with non-linear model analysis. The valuable comments from all reviewers were
329 appreciated.

330

331 **References**

332 Abdi, D., Cade-Menun, B.J., Ziadi, N., Parent, L.-É., Compositional statistical analysis of soil
333 ³¹P-NMR forms. *Geoderma*. 257–258, 40-47, 2015.

334 Anthony, W.H., Hutchinson, G.L., Livingston, G.P., Chamber measurement of soil-
335 atmosphere gas exchange: Linear vs. diffusion-based flux models. *Soil Sci. Soc. Am. J.* 59,
336 1308-1310, 1995.

337 Bai, M., 2010. Methane emissions from livestock measured by novel spectroscopic
338 techniques, School of Chemistry. University of Wollongong, p. 303.

339 Bolker, B., 2007. *Ecological Models and Data in R*. Princeton University Press, The United
340 States of America, 2007.

341 Christensen, S., Ambus, P., Arah, J.R.M., Clayton, H., Galle, B., Griffith, D.W.T.,
342 Hargreaves, K.J., Klemetsson, L., Lind, A.M., Maag, M., Scott, A., Skiba, U., Smith, K.A.,
343 Welling, M., Wienhold, F.G., Nitrous oxide emission from an agricultural field: comparison
344 between measurements by flux chamber and micrometeorological techniques. *Atmos. Environ.*
345 30, 4183, 1996.

346 Dalal, R.C., Allen, D.E., Livesley, S.J., Richards, G., Magnitude and biophysical regulators
347 of methane emission and consumption in the Australian agricultural, forest, and submerged
348 landscapes: a review. *Plant Soil*. 309, 43-76, 2008.

349 de Klein, C.A.M., Sherlock, R.R., Cameron, K.C., van der Weerden, T.J., Nitrous oxide
350 emissions from agricultural soils in New Zealand—A review of current knowledge and
351 directions for future research. *J. Roy. Soc. New Zeal.* 31, 543-574, 2001.

352 Denmead, O.T., Chamber systems for measuring nitrous oxide emission from soils in the
353 field. *Soil Sci. Soc. Am. J.* 43, 89-95, 1979.

- 354 Denmead, O.T., Novel meteorological methods for measuring trace gas fluxes. *Philos. T. R.*
355 *Soc. A.* 351, 383-396, 1995.
- 356 Denmead, O.T., Approaches to measuring fluxes of methane and nitrous oxide between
357 landscapes and the atmosphere. *Plant and Soil.* 309, 5-24, 2008.
- 358 Denmead, O.T., Chen, D., Griffith, D.W.T., Loh, Z.M., Bai, M., Naylor, T., Emissions of the
359 indirect greenhouse gases NH₃ and NO_x from Australian beef cattle feedlots. *Aust. J. Exp.*
360 *Agr.* 48, 213-218, 2008.
- 361 Denmead, O.T., Macdonald, B.C.T., Bryant, G., Naylor, T., Wilson, S., Griffith, D.W.T.,
362 Wang, W.J., Salter, B., White, I., Moody, P.W., Emissions of methane and nitrous oxide from
363 Australian sugarcane soils. *Agric. Forest Meteorol.* 150, 748-756, 2010.
- 364 Efron, B., Tibshirani, R.J., 1994. An introduction to bootstrap. Chapman&Hall/CRC, Boca
365 Raton, London, New York, Washington, D.C., 1994.
- 366 Flesch, K.T., Baron, V., Wilson, J., Griffith, D.W.T., Basarab, J., Carlson, P., Agricultural
367 gas emissions during the spring thaw: Applying a new measurement technique. *Agric. Forest*
368 *Meteorol.* 221, 111-121, 2016.
- 369 Flesch, T.K., McGinn, S.M., Chen, D.L., Wilson, J.D., Desjardins, R.L., Data filtering for
370 inverse dispersion emission calculations. *Agric. Forest Meteorol.* 198-199, 1-6, 2014.
- 371 Flesch, T.K., Prueger, J.H., Hatfield, J.L., Turbulent Schmidt number from a tracer
372 experiment. *J. Appl. Meteorol.* 111, 299-307, 2002.
- 373 Griffith, D.W.T., Synthetic calibration and quantitative analysis of gas-phase FT-IR spectra.
374 *Appl. Spectrosc.* 50, 59-70, 1996.
- 375 Griffith, D.W.T., Bryant, G.R., Hsu, D., Reisinger, A.R., Methane emissions from free-
376 ranging cattle: comparison of tracer and integrated horizontal flux techniques. *J. Environ.*
377 *Qual.* 37, 582-591, 2008.
- 378 Griffith, D.W.T., Deutscher, N.M., Caldw, C., Kettlewell, G., Riggenbach, M., Hammer, S.,
379 A Fourier transform infrared trace gas and isotope analyser for atmospheric applications.
380 *Atmos. Meas. Tech.* 5, 2481-2498, 2012.
- 381 Griffith, D.W.T., Galle, B., Flux measurements of NH₃, N₂O and CO₂ using dual beam FTIR
382 spectroscopy and the flux gradient technique. *Atmos. Environ.* 34, 1087-1098, 2000.
- 383 Hargreaves, K.J., Wienhold, F.G., Klemedtsson, L., Arah, J.R.M., Beverland, I.J., Fowler, D.,
384 Galle, B., Griffith, D.W.T., Skiba, U., Smith, K.A., Welling, M., Harris, G.W., Measurement
385 of nitrous oxide from Agricultural land using micrometeorological methods. *Atmos. Environ.*
386 30, 1563-1571, 1996.
- 387 Hutchinson, G.L., Mosier, A.R., Improved soil cover method for field measurement of
388 nitrous oxide fluxes. *Soil Sci. Soc. Am. J.* 45, 311-316, 1981.
- 389 Jones, S.K., Famulari, D., Di Marco, C.F., Nemitz, E., Skiba, U.M., Rees, R.M., Sutton,
390 M.A., Nitrous oxide emissions from managed grassland: a comparison of eddy covariance
391 and static chamber measurements. *Atmos. Meas. Tech.* 4, 2179-2194, 2011.

392 Judd, M.J., Kellier, F.M., Ulyatt, M.J., Lassey, K.R., Tate, K.R., Shelton, D., Harvey, M.J.,
393 Walker, C.F., Net methane emissions from grazing sheep. *Global Change Biol.* 5, 647-657,
394 1999.

395 Laubach, J., Kelliher, F.M., Measuring methane emission rates of a dairy cow herd by two
396 micrometeorological techniques. *Agric. Forest Meteorol.* 125, 279-303, 2004.

397 Levy, P.E., Gray, A., Leeson, S.R., Gaiawyn, J., Kelly, M.P.C., Cooper, M.D.A., Dinsmore,
398 K.J., Jones, S.K., Sheppard, L.J., Quantification of uncertainty in trace gas fluxes measured
399 by the static chamber method. *Eur. J. Soil Sci.* 62, 811-821, 2011.

400 Li, J., Tong, X., Yu, Q., Dong, Y., Peng, C., Micrometeorological measurements of nitrous
401 oxide exchange above a cropland. *Atmos. Environ.* 42, 6992-7001, 2008.

402 Matthias, A.D., Yarger, D.N., Weinback, R.S., A numerical evaluation of chamber methods
403 for determining gas fluxes. *Geophys. Res. Lett.* 5, 765-768, 1978.

404 Neftel, A., Ammann, C., Fischer, C., Spirig, C., Conen, F., Emmenegger, L., Tuzson, B.,
405 Wahlen, S., N₂O exchange over managed grassland: Application of a quantum cascade laser
406 spectrometer for micrometeorological flux measurements. *Agric. Forest Meteorol.* 150, 775-
407 785, 2010.

408 Norman, J.M., Kucharik, C.J., Gower, S.T., Baldocchi, D.D., Crill, P.M., Rayment, M.,
409 Savage, K., Striegl, R.G., A comparison of six methods for measuring soil-surface carbon
410 dioxide fluxes. *J. Geophys. Res.* 102, 28771-28777, 1997.

411 Pattey, E., Strachan, I.B., Desjardins, R.L., Edwards, G.C., Dow, D., MacPherson, J.I.,
412 Application of a tunable diode laser to the measurement of CH₄ and N₂O fluxes from field to
413 landscape scale using several micrometeorological techniques. *Agric. Forest Meteorol.* 136,
414 222-236, 2006.

415 Ruser, R., Flessa, H., Schilling, R., Steindl, H., Beese, F., Soil compaction and fertilization
416 effects on nitrous oxide and methane fluxes in potato fields. *Soil Sci. Soc. Am. J.* 62, 1587-
417 1595, 1998.

418 Sommer, S.G., McGinn, S.M., Hao, X., Larney, F.J., Techniques for measuring gas emissions
419 from a composting stock pile of cattle manure. *Atmos. Environ.* 38, 4643-4652, 2004.

420 Turner, D.A., Chen, D., Galbally, I.E., Leuning, R., Edis, R.B., Li, Y., Kelly, K., Phillips, F.,
421 Spatial variability of nitrous oxide emissions from an Australian irrigated dairy pasture. *Plant
422 and Soil.* 309, 77-88, 2008.

423 Venterea, R.T., Theoretical comparison of advanced methods for calculating nitrous oxide
424 fluxes using non-steady state chambers. *Soil Sci. Soc. Am. J.* 77, 709-720, 2013.

425 Venterea, R.T., Dolan, M., Ochsner, T.E., Urea decreases nitrous oxide emissions compared
426 with anhydrous ammonia in a Minnesota corn cropping system. *Soil Sci. Soc. Am. J.* 74, 407-
427 418, 2010.

428 Wang, K., Zheng, X., Pihlatie, M., Vesala, T., Liu, C., Haapanala, S., Mammarella, I.,
429 Rannik, Ü., Liu, H., Comparison between static chamber and tunable diode laser-based eddy

430 covariance techniques for measuring nitrous oxide fluxes from a cotton field. *Agric. Forest Meteorol.* 171–172, 9-19, 2013.

431

432 Webb, E.K., Pearman, G.I., Leuning, R., Correction of flux measurements for chemistry
 433 effects due to heat and water vapour transfer. *Quart. J. R. Meteorol. Soc.* 106, 85-100, 1980.

434 Wilson, J.D., Flesch, T.K., Generalized flux-gradient technique pairing line-average
 435 concentrations on vertically separated paths. *Agric. Forest Meteorol.* 220, 170-176, 2016.

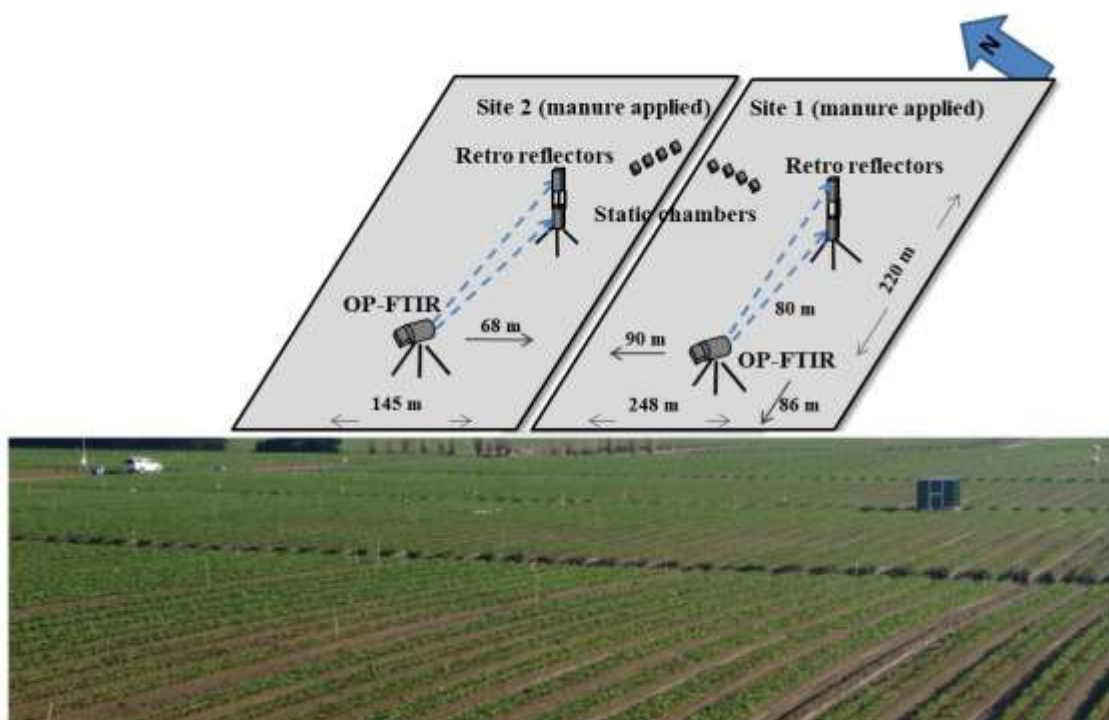
436 Yao, Z., Zheng, X., Xie, B., Liu, C., Mei, B., Dong, H., Butterbach-Bahl, K., Zhu, J.,
 437 Comparison of manual and automated chambers for field measurements of N₂O, CH₄, CO₂
 438 fluxes from cultivated land. *Atmos. Environ.* 43, 1888-1896, 2009.

439

440 **Figures**

441 Figure 1

442

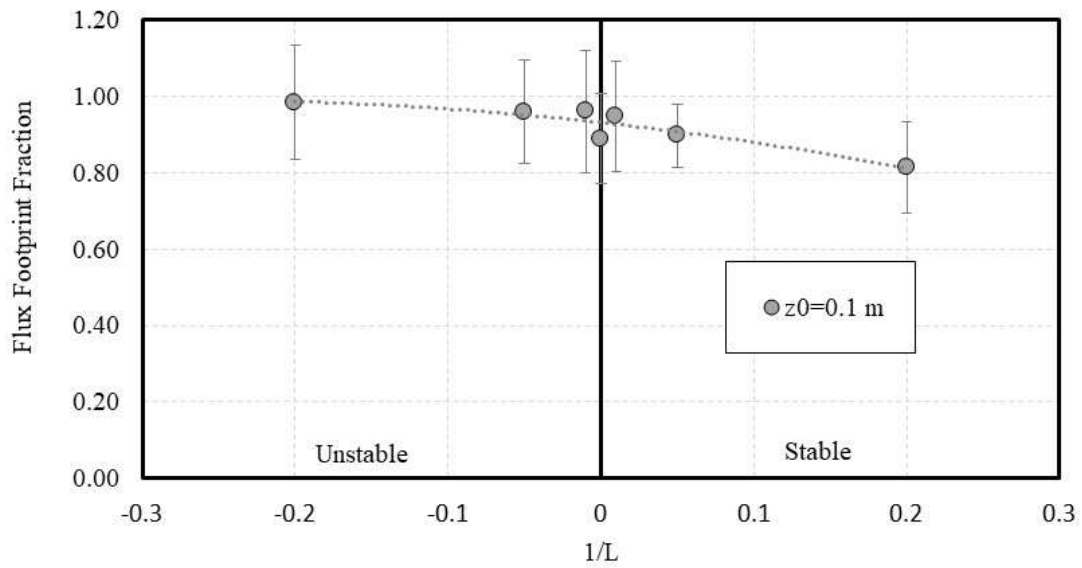


443

444 **Figure 1** The design of the study (upper panel) and photo of experimental site with OP-FTIR
 445 set up (lower panel). Emission measurements were conducted with static chambers (four per
 446 site) and FG using the OP-FTIR spectroscopy system with retro reflectors at 0.8 and 1.8 m
 447 above ground. The figure is not in scale.

448

449 Figure 2

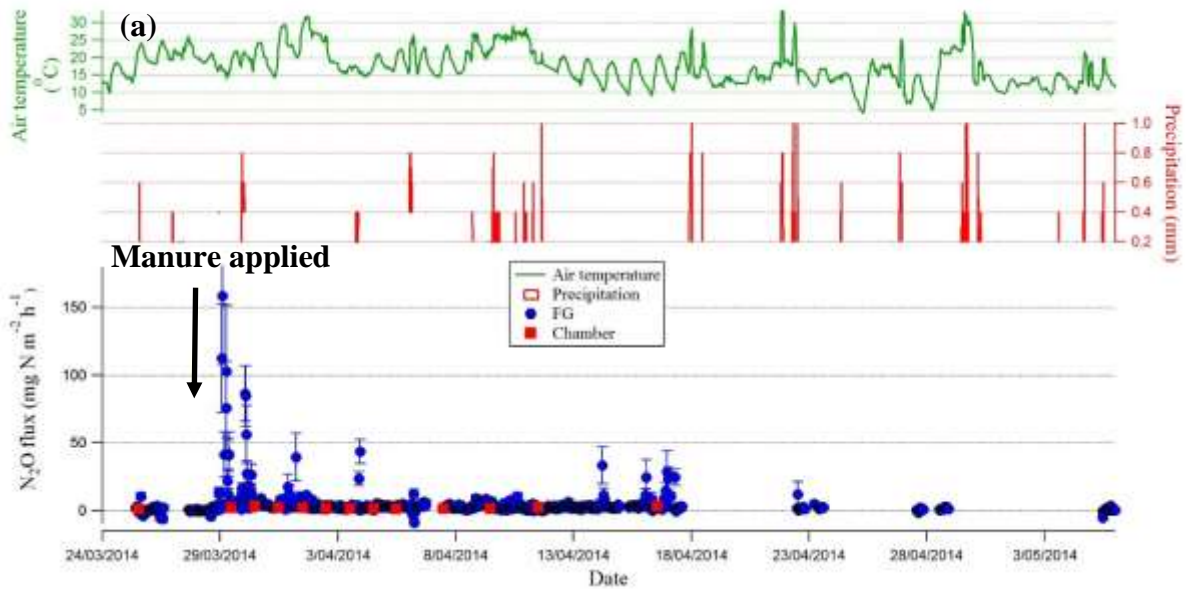


450

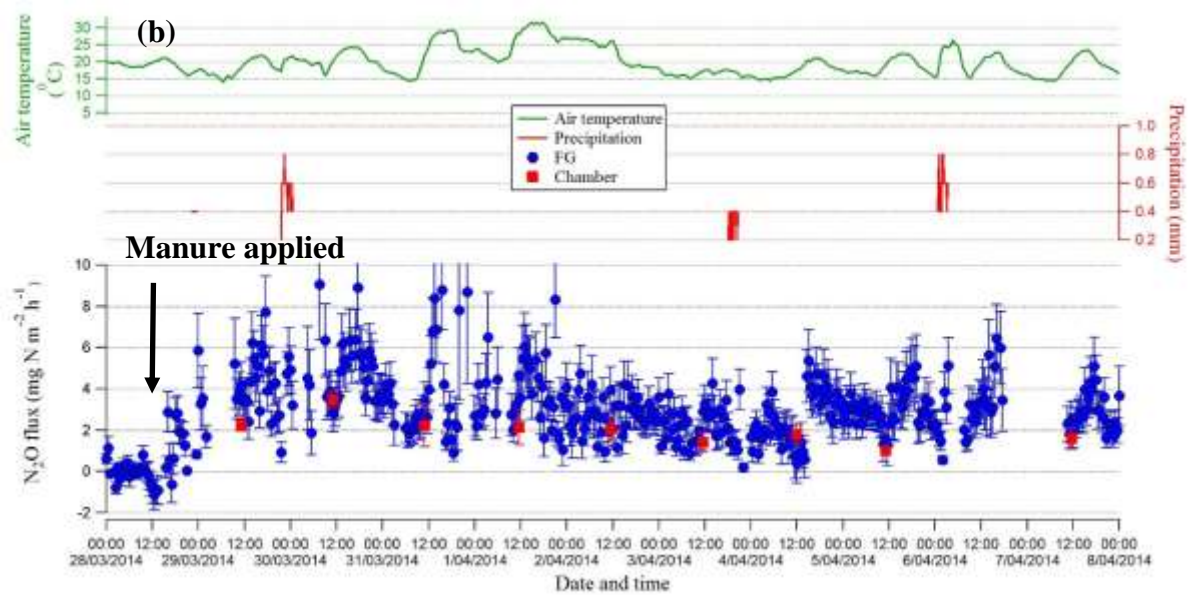
451 **Figure 2** Estimated flux footprint fraction at Site 2, plotted versus atmospheric stability (the
452 reciprocal of the Obukhov length L). The model results are for a roughness length $z_0 = 0.1$ m.

453

454 Figure 3



455



456

457 **Figure 3** (a) Hourly N₂O fluxes measured by FG and static chambers from 25 March to 6 May.

458 Air temperature and precipitation are plotted during the same period; and (b) subset of N₂O

459 fluxes from 28 March to 8 April. Error bars (both upper and lower panels) represent 1- σ

460 estimate of measurement uncertainty ($\delta_{Q_{FG}}$) for the FG measurements and standard error for

461 chambers. Manure was applied on 28 March 2014.